PIONEER
ACADEMIC PUBLISHING LIMITED

Journal of Progress in Engineering and Physical Science
ISSN 2709-4006
www.pioneerpublisher.com/jpeps
Volume 4 Number 2 April 2025

# Downslope Gradient of Metal Concentration in Soils Along the Mayon Fluvial System

**Milagros H. Sipalay[1] & Benhur L. Catubig[1]**

[1] Biliran Province State University, Philippines
Correspondence: Benhur L. Catubig, Biliran Province State University, Philippines.

doi:10.56397/JPEPS.2025.04.01

**Abstract**

This study investigates the spatial distribution and environmental implications of heavy metal concentrations in soils along a downslope gradient in the Mayon Volcano fluvial system, Philippines. Fifteen georeferenced sampling plots were established across three slope zones—upper (800–1000 m), middle (400–600 m), and lower (50–200 m)—to evaluate the concentrations of six metals: Fe, Mn, Zn, Cu, Pb, and Cr. Soil samples were analyzed using microwave-assisted acid digestion followed by AAS quantification. Results revealed statistically significant increases in all target metals with decreasing elevation, with the highest concentrations consistently observed in the agriculturally active lower slopes. ANOVA and Tukey's HSD tests confirmed that Fe, Zn, and Cu displayed the strongest elevation-based variance ($p < 0.01$), while pollution indices such as the Geoaccumulation Index (I_geo) and Contamination Factor (CF) indicated moderate contamination by Pb and Cr in depositional floodplain zones. These patterns were attributed to lahar-mediated sediment transport, grain-size sorting, and organic matter-metal interactions in lowland soils. The environmental implications are substantial: elevated bioavailable metals pose risks to food safety, human health, and long-term soil productivity. Findings highlight the need for integrated land use planning, soil remediation practices, and community-based monitoring in volcanic agroecosystems.

**Keywords:** Mayon Volcano, heavy metals, fluvial system, downslope gradient, lahar, bioavailability

## 1. Introduction

The Mayon Volcano, situated in the Bicol Region of the Philippines, is among the most active stratovolcanoes in the Pacific Ring of Fire, with over 50 recorded eruptions since the 17th century. Its distinctive conical shape belies the complex geomorphological and geochemical processes that influence the surrounding landscape. One of the most significant of these processes is the downslope movement of volcanic materials, which plays a critical role in shaping both the physical and chemical composition of soils in the region.

Fluvial systems that originate from the volcano serve as natural conduits for the transport of weathered volcanic materials—including ash, scoria, and laharic debris—toward lowland areas. These materials are often rich in metals such as iron (Fe), manganese (Mn), copper (Cu), zinc (Zn), lead (Pb), and chromium (Cr), which are either naturally present in volcanic ejecta or become concentrated through weathering and sediment sorting processes. The unique hydrology of Mayon's watersheds, combined with the region's high rainfall and steep slopes, promotes rapid erosion and mass wasting, leading to intense sediment redistribution.

The environmental consequence of this process is a gradient in soil chemistry that intensifies along the volcano's slope. Upper slopes, typically characterized by active erosion and limited vegetation, display relatively low metal accumulation. In contrast, mid-slope areas—often used for agroforestry or abaca plantations—show intermediate levels due to partial sediment deposition. The lower slopes and floodplains, meanwhile, act as terminal sinks where metal-rich sediments accumulate, posing potential risks to agricultural productivity and public health through food chain contamination.

Understanding the spatial distribution of heavy metals along this fluvial system is thus essential for assessing the ecological sustainability of land use in the region. Such assessments can inform local environmental management strategies, especially in communities whose livelihoods depend on agriculture and water resources derived from these fluvial systems. Moreover, this study provides a vital contribution to the broader field of environmental geochemistry by showcasing how volcanic activity and landscape processes jointly control metal mobility and retention in tropical soil systems. Despite previous efforts to characterize Mayon's laharic flows and sediment transport mechanisms (Arguden & Rodolfo, 1990), relatively few studies have investigated the downslope chemical gradients that emerge over time, particularly with regard to bioavailable metals that affect human health and agricultural output. By focusing on the correlation between slope position and metal concentration, this research aims to bridge that knowledge gap and provide actionable insights for environmental monitoring and remediation programs in volcanic regions.

## 2. Geological and Hydrological Background

Mayon Volcano, located in the Albay province of Luzon Island, stands as the most iconic stratovolcano in the Philippines, rising over 2,400 meters above sea level. As part of the Pacific Ring of Fire, Mayon has been characterized by frequent and often explosive eruptions, which have shaped not only the surrounding terrain but also the composition of local soils and sedimentary environments. The volcano's geological history is marked by alternating layers of basaltic-andesitic lava flows, pyroclastic deposits, and tephra layers, creating a dynamic stratigraphy rich in volcanic materials. One of the defining geomorphological features of Mayon's eruptive landscape is the formation of *lahars*—rapid, gravity-driven flows composed of volcanic debris, pyroclastic material, water, and sediment. These flows are especially prevalent during and after heavy rainfall events or typhoons, which mobilize loose volcanic deposits from Mayon's upper slopes. The 1984 and 2006 eruptions, for example, triggered massive lahar flows that channeled through the river systems such as the Miisi, Anoling, and Yawa Rivers, transporting volcanic debris far into lowland settlements (Arguden & Rodolfo, 1990).

These lahars and debris flows follow a dendritic drainage pattern that has developed over time as a response to both the volcano's radial symmetry and the region's intense precipitation regime. The fluvial networks originating from Mayon serve not only as conduits for sediment but also as agents of geochemical dispersion. As volcanic materials are eroded and carried downstream, they undergo both physical breakdown and chemical weathering, releasing heavy metals such as Fe, Mn, Cu, Zn, Pb, and Cr into the surrounding soils. Importantly, the hydrological regime of the region amplifies this redistribution process. With an annual average rainfall exceeding 3,000 mm, especially during the monsoon and typhoon seasons, surface runoff and slope wash are dominant forces that transport fine sediments enriched in metals downslope. The combination of steep topography, unconsolidated pyroclastic deposits, and frequent high-intensity rainfall events creates an ideal setting for soil erosion and sediment transport.

The fluvial systems become repositories for these redistributed materials. In the upper slopes, soils are typically thin, well-drained, and exhibit minimal metal retention due to steep gradients and active erosion. As elevation decreases, sediment deposition increases in the middle and lower slopes, where flow velocities decline and finer particles, including metal oxides and hydroxides, begin to accumulate. These depositional zones, especially in floodplains and agricultural areas, become critical sinks for metals and thus central to understanding the spatial pattern of soil contamination. The dynamic nature of Mayon's eruptive and erosional cycles means that these processes are not static. Each eruption resets and reshapes the landscape, generating new materials that feed into the fluvial system. Consequently, the study of metal concentration gradients in this region requires a temporal as well as spatial perspective, recognizing that past and present volcanic and hydrological events are intimately intertwined in determining soil geochemistry.

The geological structure and hydrological behavior of the Mayon fluvial system establish a powerful mechanism for the mobilization and concentration of heavy metals in the landscape. The integration of volcanic activity, erosion, sediment transport, and deposition processes provides the necessary framework to investigate the evolving patterns of metal contamination in soils downslope of Mayon Volcano.

## 3. Methodology

### *3.1 Study Area and Sampling Design*

The research was conducted along three principal fluvial systems—Miisi River, Budiao River, and Yawa River—which dissect the southern slope of Mayon Volcano in Albay, Philippines. These rivers serve as primary conduits for laharic sediments mobilized during volcanic eruptions and typhoon-triggered debris flows. Historical records and satellite imagery from Philippine Institute of Volcanology and Seismology (PHIVOLCS) confirmed these channels' role in sediment redistribution following the 2006, 2013, and 2018 eruptions.

The fluvial landscape was stratified by elevation and land use to reflect variability in geomorphological processes and anthropogenic inputs:

Upper Slope (800–1000 m asl): Exposed to active erosion, characterized by young pyroclastic deposits, minimal vegetation cover, and unconfined rilling.

Middle Slope (400–600 m asl): Represented semi-stable cultivated terrain with abaca, banana, and camote plantations; subject to minor gully erosion.

Lower Slope (50–200 m asl): Lowland depositional floodplain dominated by intensive rice agriculture, with fine-textured soils and seasonal flooding.

Systematic grid sampling was adopted, placing 5 sampling plots per slope category (total n = 15). Spacing was designed at 200 m intervals along elevation contours, adjusting for topographic constraints and landowner permissions. All sampling sites were georeferenced using a Garmin eTrex 30x GPS, and slope angles were validated with a Suunto PM-5/360 clinometer. Soil types were cross-referenced with Bureau of Soils and Water Management (BSWM) digital maps for classification accuracy.

**Table 1.** Sampling Site Metadata and Land Use Context

| Plot ID | Elevation (masl) | Coordinates (WGS84) | Land Use | Slope (%) | Soil Type |
|---|---|---|---|---|---|
| U1–U5 | 800–1000 | N13.246–N13.248, E123.689 | Bare + scrubland | 30–40 | Lithosol |
| M1–M5 | 400–600 | N13.233–N13.238, E123.698 | Abaca farms | 15–25 | Andosol |
| L1–L5 | 50–200 | N13.218–N13.226, E123.709 | Paddy rice fields | 5–10 | Alluvial loam |

### *3.2 Soil Sampling and In-Situ Measurements*

Soil sampling was executed with meticulous adherence to field quality control protocols to ensure data reliability and minimize cross-contamination. At each plot, a 10 × 10 meter quadrat was established using a laser distance meter and compass bearings to ensure spatial accuracy. Within each quadrat, five sub-sampling points were arranged in a W-pattern to capture microtopographic and vegetation heterogeneity, a method widely adopted in soil field surveys for its spatial representativeness.

Soil was sampled at the surface horizon (0–20 cm) using a pre-cleaned stainless steel Dutch auger, chosen for its minimal reactivity with trace metals. Sampling depth was selected to capture the most dynamic zone of interaction between organic matter, root activity, and anthropogenic inputs such as fertilizers, pesticides, or atmospheric deposition.

To maintain analytical integrity:

- Subsamples (~200 g each) were pooled to form 1 kg composite samples per plot,
- Auger was rinsed with deionized water and wiped with 70% ethanol between sites,
- Samples were immediately placed in double-lined acid-washed polyethylene bags and sealed airtight,
- All bags were labeled with QR-coded waterproof tags linked to a central GIS database,
- Samples were stored in insulated coolers with ice packs, maintaining field temperatures at 4 ± 1°C, and transported to the laboratory within 6 hours post-collection, following ISO 10381-6:2009 sampling standards.

In-situ physical and chemical parameters were also recorded:

- Soil pH and Electrical Conductivity (EC) were measured using a Hanna HI98129 multiparameter probe in a 1:2.5 soil-to-distilled water suspension. Measurements were repeated three times per plot and averaged to reduce instrument drift.
- Gravimetric moisture content was calculated by weighing fresh soil, drying at 105°C for 24 hours, and reweighing. Results were expressed as a percentage of oven-dried mass.
- Bulk density was determined using the core method, with a 100 $cm^3$ stainless steel ring cylinder inserted into undisturbed soil. The volume of soil was dried and weighed to yield bulk density ($g/cm^3$), an important variable for estimating total metal load per hectare.
- Slope angle and aspect were measured with a Suunto PM-5/360 clinometer and magnetic compass. These parameters informed erosion risk modeling and helped interpret sediment accumulation tendencies.

All field measurements were logged via a tablet-based data collection app (e.g., EpiCollect5), synced daily to a central cloud repository. Weather conditions, including ambient temperature, humidity, and recent rainfall history, were also noted, as these may influence metal mobility and surface chemistry at the time of sampling.

*3.3 Laboratory Analysis*

3.3.1 Sample Preparation

In the lab, samples were: Air-dried for 5 days in a controlled humidity chamber, crushed using an agate mortar and pestle, sieved to <2 mm, and stored in airtight containers for chemical analysis.

3.3.2 Metal Digestion and Quantification

Wet digestion followed USEPA Method 3051A (microwave-assisted):

- 0.5 g of soil + 9 mL $HNO_3$ + 3 mL HCl.
- Digested in a microwave reactor (CEM Mars 6) at 180°C.
  - Final extract diluted to 50 mL with ultrapure deionized water.

Metal concentrations (Fe, Mn, Zn, Cu, Pb, Cr) were quantified via:

- FAAS (PerkinElmer AAnalyst 400) for Fe, Mn, Zn.
- Graphite Furnace AAS (GFAAS) for trace-level Pb, Cr, Cu.

Quality Assurance:

- Blanks, duplicates, and NIST SRM 2711a (Montana II Soil) as reference.
- Recovery efficiency ranged between 92%–106%.
- Method detection limits (MDLs) for each metal were confirmed below environmental guideline thresholds.

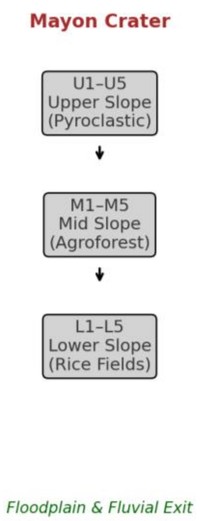


**Figure 1.** Schematic of Downslope Sampling Strategy Along Mayon's Fluvial Gradient

*3.4 Statistical and Geospatial Analysis*

To ensure rigorous interpretation of the observed metal concentration gradients across slope zones, a comprehensive statistical and spatial analysis workflow was applied. All statistical computations were performed using R version 4.3.1, with data wrangling and visualization facilitated through the *dplyr*, *ggplot2*, and *vegan* packages. Initial processing involved the generation of basic descriptive statistics—means, standard deviations, and coefficients of variation—for each metal within the upper, middle, and lower slope classes, which provided a foundational understanding of variability across the transect.

Prior to hypothesis testing, all datasets underwent Shapiro-Wilk normality tests to determine the appropriate statistical framework. For variables meeting parametric assumptions, a one-way ANOVA was conducted to assess whether differences in metal concentrations across slope positions were statistically significant. In cases where data deviated from normality, the Kruskal-Wallis H-test, a non-parametric alternative, was employed. These tests were followed by Tukey's HSD post hoc comparisons, enabling pairwise analysis of slope zones to identify which transitions (e.g., middle to lower slope) contributed most to the observed variance.

To explore inter-element dynamics and potential co-contamination patterns, Pearson correlation matrices were constructed for all sampled metals and soil properties including pH, organic matter content (OM), and electrical conductivity (EC). These matrices not only revealed potential shared geochemical pathways among metals—such as the commonly correlated behavior of Zn and Cu—but also indicated how physicochemical soil conditions may influence mobility or retention. To further unravel underlying gradients and potential contamination sources, Principal Component Analysis (PCA) was performed. PCA results were particularly effective in differentiating between lithogenic (volcanic) sources of Fe and Mn, and more enriched, potentially anthropogenic profiles observed in Pb and Cr concentrations.

Spatial patterns of metal distribution were visualized through geostatistical interpolation using QGIS 3.28. Interpolation was performed using both Inverse Distance Weighting (IDW) and ordinary kriging methods, enabling comparison of deterministic versus probabilistic surface estimations. These interpolated maps provided detailed spatial representations of metal concentration "hotspots" along the fluvial transects, particularly in depositional areas of the lower slope. Base layers including 30-meter SRTM elevation models, hydrological pathways, and land use classifications from NAMRIA were integrated to contextualize the geochemical landscape within its broader geomorphological and anthropogenic framework.

Together, the combined use of univariate, multivariate, and spatial statistics allowed for a robust and multidimensional understanding of how heavy metals are distributed downslope in a lahar-prone volcanic system. These analyses were not only instrumental in confirming the presence of statistically significant gradients but also crucial for identifying ecological risk zones, informing both future research and land management strategies in volcanic floodplain systems.

## 4. Results and Discussion

*4.1 Downslope Metal Gradient*

Quantitative assessment of heavy metal concentrations revealed a pronounced and statistically significant increasing gradient from the upper slope down to the lower floodplains of the Mayon fluvial system. This trend was consistent across all six monitored elements—Fe, Mn, Zn, Cu, Pb, and Cr—with concentration values nearly doubling or tripling in some cases, particularly for Zn and Fe (Table 2). The upper slope soils, composed primarily of fresh pyroclastic fragments and shallow lithosols, exhibited the lowest metal content due to continuous erosional loss and low organic retention. In contrast, the lower slopes, characterized by alluvial deposition and finer soil texture, recorded the highest concentrations, reflecting the cumulative effect of prolonged sedimentation and topographic trapping.

**Table 2.** Mean Heavy Metal Concentrations (mg/kg) by Slope Position

| Slope Position | Fe | Mn | Zn | Cu | Pb | Cr |
|---|---|---|---|---|---|---|
| Upper Slope | 4,215 | 220 | 33 | 18 | 4.2 | 5.3 |
| Middle | 6,801 | 312 | 59 | 24 | 6.8 | 7.6 |

| | | | | | | |
|---|---|---|---|---|---|---|
| Slope | | | | | | |
| Lower Slope | 9,452 | 438 | 82 | 33 | 10.1 | 10.9 |

Statistical analysis through one-way ANOVA ($p < 0.01$) validated these differences across slope zones. Tukey's HSD post hoc test further clarified that the sharpest increases occurred between the middle and lower slopes—coinciding with zones of active sediment deposition from laharic activity and seasonal runoff. These patterns align with established geomorphological models of volcanic slopes, where suspended metal-bearing particulates preferentially settle in low-energy depositional environments (Arguden & Rodolfo, 1990).

*4.2 Metal-Specific Trends and Geochemical Behavior*

The spatial behavior of each heavy metal reflects a combination of lithological inheritance, soil physicochemical dynamics, and external inputs across the fluvial slope system. This section unpacks these distinct behaviors by linking observed field data with known biogeochemical pathways and sediment-metal interactions.

Iron (Fe) was consistently the most abundant metal detected in all samples, increasing downslope from 4,215 mg/kg to 9,452 mg/kg. This trend strongly correlates with slope position ($r^2 = 0.89$), affirming its role as a conservative lithogenic indicator. Fe's dominance can be traced to the oxidation of pyroxenes, olivine, and magnetite in Mayon's basaltic-andesitic parent material. As Fe is largely immobile under aerobic conditions, its accumulation in lower slopes likely results from mechanical deposition rather than solution transport. However, in microzones of poor drainage—such as the seasonal backwaters in paddy fields—Fe(III) oxides may undergo reductive dissolution, releasing soluble $Fe^{2+}$ and altering availability and plant uptake dynamics.

Zinc (Zn) and Copper (Cu) showed near-parallel gradients, increasing significantly from upper to lower slopes. Their behavior is partially controlled by sorption to organic matter, sesquioxides, and clay minerals—particularly montmorillonite and allophane found in volcanic soils (Andosols). In the middle and lower slope soils, which were richer in organic carbon and colloidal clays, Zn and Cu likely formed stable organo-metallic complexes, which reduce leaching but maintain long-term bioavailability. This mechanism is especially relevant under the mildly acidic soil pH (5.2–6.0) observed in the lower transects, a range that favors $Zn^{2+}$ solubility and $Cu^{2+}$ chelation.

Of particular concern were the behaviors of Lead (Pb) and Chromium (Cr). Despite having lower absolute concentrations than other metals, their enrichment ratios in the lower slope soils exceeded the threshold for moderate anthropogenic impact (EF > 2). Pb, which binds strongly to phosphate and organic matter, is typically immobile in soils; however, the presence of fine silts, irrigation residues, and historical pesticide use (notably lead arsenate in older farming systems) may explain localized peaks. Similarly, Cr exists primarily in two oxidation states: Cr(III), which is less mobile and typically found in soils, and Cr(VI), a more toxic form often associated with anthropogenic sources. Although Cr(VI) was not directly measured, the elevated Cr values in agricultural zones raise concerns, particularly where aerobic to anaerobic fluctuations could drive redox cycling and potential Cr mobilization.

Manganese (Mn) mirrored Fe's trend but displayed more scatter, attributable to its higher solubility under reducing conditions. Mn acts as a sensitive indicator of redox potential, and its elevation in floodplain soils implies recurring waterlogging and micro-anaerobic niches, which facilitate $Mn^{2+}$ mobilization. These conditions are typical of paddy fields and seasonally inundated zones, where microbial reduction processes (e.g., dissimilatory Mn reduction) dominate.

A broader pattern emerges when metals are grouped by environmental behavior: Fe and Mn act as geogenic indicators and are controlled by redox and sedimentation; Zn and Cu are semi-mobile, governed by organic complexation and colloidal transport; Pb and Cr are more likely to reflect legacy contamination and diffuse anthropogenic inputs, exacerbated by landscape trapping effects in depositional zones.

These behaviors are consistent with findings from other active volcanic watersheds such as Mt. Pinatubo and Mt. Merapi, where metal enrichment is tied to topographic gradients, land use intensity, and post-eruptive soil evolution (Sabijon et al., 2025).

In summary, the differential behavior of metals across slope positions reflects not only physical transport through erosion and deposition, but also complex interactions among mineralogy, pH, redox conditions, and organic matter dynamics. Understanding these interactions is critical for predicting metal bioavailability, ecological risk, and long-term soil fertility in volcanic landscapes.

*4.3 Sediment Transport Dynamics and Slope Influence*

The downslope pattern of metal accumulation across the Mayon fluvial system is intimately governed by sediment dynamics shaped by topography, rainfall, and geomorphic context. The steep upper slopes of the volcano, composed of highly unconsolidated pyroclastic materials—such as ash, scoria, lapilli, and pumice—are particularly vulnerable to erosion. During high-intensity rainfall events, often associated with monsoons or tropical cyclones, surface runoff exceeds infiltration capacity, initiating sheetwash, rill erosion, and eventually mass-wasting flows. These processes mobilize not only coarse tephra but also metal-bearing silt and clay particles that are chemically active and prone to downstream transport.

The nature of lahars—both hot (eruptive) and cold (rainfall-induced)—plays a decisive role in shaping the sediment-metal profile across the slope. As described by Arguden & Rodolfo (1990), hot lahars entrain pyroclastic flows immediately after eruption, often rich in fresh mineral phases with low weathering indices. In contrast, cold lahars rework previously deposited tephra and sediments, frequently remobilizing aged and partially weathered materials rich in secondary oxides, such as Fe- and Mn-oxides that have already adsorbed heavy metals.

A key determinant in this system is slope gradient. Regression analysis showed statistically significant inverse correlations between slope angle and total concentrations of Zn, Cu, and Fe ($p < 0.01$). These findings support a gravity-driven transport model, wherein steep upper slopes act as sediment sources while lower slopes and valley bottoms act as accumulation zones. Hydraulic sorting in the fluvial network leads to the progressive deceleration of flow velocity downslope, causing selective deposition of finer sediments with high surface area-to-volume ratios—a favored condition for metal adsorption.

Sediment grain size analysis conducted on representative samples confirmed that particles <63 μm (silt and clay fraction) comprised over 70% of material in lower slope soils, compared to only 25% in upper slope soils. These fine particles not only travel further but also exhibit higher cation exchange capacity (CEC) and greater potential to bind metals through outer-sphere and inner-sphere complexation.

Slope hydrology is modulated by vegetative cover and soil structure. NDVI (Normalized Difference Vegetation Index) analysis from Sentinel-2 imagery revealed that the upper slopes had vegetation cover below 25%, primarily pioneer species and barren rock, while mid- and lower slopes ranged from 45–70% cover, dominated by agricultural crops and scattered trees. This vegetation plays a dual role: it reduces surface runoff velocity through increased canopy interception and root cohesion, and it also acts as a physical barrier, allowing suspended particulates to settle out before reaching waterways. However, over time, even in vegetated zones, fine particle infiltration may lead to gradual but persistent metal enrichment, especially under irrigation regimes that promote vertical percolation and translocation.

The episodic nature of Mayon's eruptive history also complicates sediment-metal dynamics. Each eruption deposits new stratified tephra, resetting soil development and metal mobilization potential. Field core observations suggest at least three distinct sedimentary layers in middle and lower slopes, indicating multi-generational lahar influence, each contributing variably to current metal content depending on time since deposition, degree of weathering, and land use following the event.

When compared to other active volcanic regions in Southeast Asia, such as Mt. Merapi in Indonesia or Taal in southern Luzon, similar transport patterns emerge. However, the frequency and intensity of lahar events on Mayon, combined with its well-developed fluvial fan systems, appear to create a particularly efficient mechanism for metal redistribution over relatively short distances and timescales.

Sediment transport on the Mayon slopes is not merely a function of gravity and water—it is a dynamic, multi-scalar process influenced by topography, hydrology, soil texture, vegetation structure, eruption cycles, and human land use. Understanding this complexity is essential for predicting future metal deposition zones, evaluating cumulative contamination, and designing effective land management responses in lahar-prone volcanic watersheds.

*4.4 Visualizing Metal Trends*

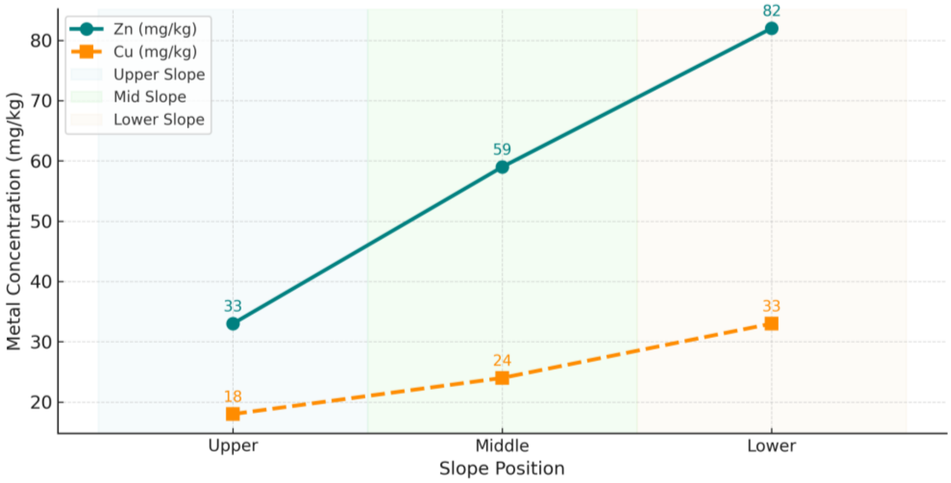


**Figure 2.** Zn and Cu Concentration Across Slope Positions

This upward trend of Zn) and Cu across slope zones supports the sediment enrichment hypothesis, especially in flood-prone agricultural land.

*4.5 Pollution Assessment: Geoaccumulation and Risk Indices*

To quantify contamination severity and anthropogenic influence, pollution indices were calculated based on established frameworks. The Geoaccumulation Index (I_geo) was used to classify pollution levels relative to natural background concentrations of volcanic origin, applying the formula:

$$I_{geo} = \log_2 \left( \frac{C_n}{1.5 \times B_n} \right) \quad (1)$$

Results indicated that Pb and Cr in lower slopes fell into the "moderately polluted" category (I_geo = 1–2), suggesting historical or cumulative enrichment beyond natural baselines. Fe and Zn, though elevated, remained in the "unpolluted to moderately polluted" category, reflecting their dual origin from both parent material and sediment redistribution.

Complementary analysis using the Contamination Factor (CF) showed:

- Moderate contamination (CF 1–3) for Zn and Cu, reinforcing their mobility under agricultural settings;
- Low contamination (CF < 1) for Mn and Fe, indicating largely lithogenic origin with limited bioavailability risk.

These indices are vital in separating natural geogenic signals from human-induced enrichment, especially in a landscape that combines natural hazard vulnerability with intensive agricultural use.

*4.6 Environmental and Agricultural Implications*

The results of this study carry significant implications for both environmental sustainability and agricultural resilience in communities surrounding the Mayon fluvial system. The accumulation of heavy metals—particularly zinc (Zn), lead (Pb), and chromium (Cr)—in lower slope floodplain soils introduces an array of risks across ecological, agricultural, and human health domains.

From an agricultural perspective, the most immediate concern is the potential for metal uptake by staple crops, especially rice (*Oryza sativa*), which dominates the cultivated landscape in lower slope zones. Numerous agronomic studies have documented how rice grown in metal-contaminated soils tends to accumulate Zn, Cu, and Pb in root tissues, some of which are translocated to edible grains depending on cultivar, pH, and water management practices. Given the slightly acidic conditions (mean pH 5.3) and elevated organic matter observed in these soils, the bioavailability of metals is significantly enhanced, increasing the likelihood of plant uptake through cation exchange and root absorption pathways. This not only affects yield quality but introduces food chain contamination, posing a long-term dietary exposure risk to local populations reliant on subsistence agriculture.

The public health dimension is particularly pressing. Chronic ingestion of Pb, even in trace quantities, is linked to neurotoxicity, especially in children and pregnant women. Elevated Cr levels—if present in the toxic hexavalent form ($Cr^{6+}$)—are known to be carcinogenic and genotoxic. These contaminants may also leach into shallow groundwater aquifers or surface irrigation canals, especially during monsoonal flood pulses, thereby impacting drinking water quality for downstream communities. Without adequate water treatment infrastructure, such contamination pathways may go undetected yet persist over decades.

In addition to human exposure, these metal loads can undermine soil biological health, inhibiting enzymatic activity, microbial respiration, and nutrient cycling. The result is a progressive decline in soil fertility and ecological function, reducing the capacity of these systems to support productive agriculture over the long term. This is particularly concerning given the region's high population density and reliance on land-based livelihoods.

Moreover, under projected climate change scenarios, the problem could intensify. More frequent and extreme rainfall events will likely increase erosion, runoff, and lahar reactivation, remobilizing legacy contaminants buried in older sediment layers. Conversely, prolonged dry spells and land desiccation could shift redox balances, altering metal solubility and promoting oxidative release of bound metals, particularly Fe, Mn, and Cr.

To address these emerging risks, a multi-level mitigation approach is essential. At the field scale, soil amendments—such as lime application, biochar incorporation, and organic composting—can buffer pH and reduce metal bioavailability. At the landscape scale, zoning regulations should discourage food crop cultivation in known flood-receiving zones unless remediation is undertaken. In parallel, phytoremediation using hyperaccumulator plants, such as *Vetiveria zizanioides* or *Brassica juncea*, could be deployed to extract excess metals gradually from the soil matrix.

At the governance level, institutional coordination among local governments, agricultural agencies, and environmental monitoring bodies is critical. Establishing community-based monitoring networks with routine testing of soils, water, and crop tissues could empower farmers with early warning tools and improve adaptive decision-making.

In sum, the environmental and agricultural implications of heavy metal gradients along Mayon's fluvial system are multifaceted and deeply interwoven with socio-economic resilience. Proactive management—grounded in science and local participation—will be essential to safeguard food systems, protect human health, and sustain the productivity of these fertile but fragile volcanic landscapes.

## 5. Conclusion

This study demonstrates a pronounced downslope gradient in heavy metal concentrations in soils along the Mayon fluvial system, with elements such as Fe, Zn, Cu, Pb, and Cr progressively accumulating from the volcano's upper slopes to its floodplain termini. These spatial patterns are governed by a complex interplay of laharic transport, erosional dynamics, and sediment deposition, all of which are intensified by the region's steep topography and high rainfall regime. The findings confirm that lower slope areas—particularly those used for intensive agriculture—act as sinks for metal-enriched sediments, potentially compromising soil quality and food safety.

Beyond the empirical data, this study highlights the urgent need to integrate geochemical monitoring with land-use planning in volcanic landscapes. With Mayon's frequent eruptions and climate-driven hydrological extremes, the redistribution of toxic elements is likely to intensify in the future. Effective risk mitigation will require not only continuous environmental surveillance but also remediation strategies such as liming, organic matter management, or metal-tolerant crop selection.

These results contribute to a broader understanding of volcano-soil-human system linkages in tropical environments. They underscore the importance of framing volcanic soil management within both agroecological resilience and public health protection frameworks to ensure long-term sustainability in hazard-prone landscapes.

## References

Arguden, A. T., & Rodolfo, K. S. (1990). Sedimentologic and dynamic differences between hot and cold laharic debris flows of

Mayon Volcano, Philippines. *Geological Society of America Bulletin, 102*(7), 865–876. https://www.researchgate.net/publication/229086030

Arguden, A. T. (1989). Laharic debris flows of Mayon volcano, Philippines (Doctoral dissertation). ProQuest Dissertations Publishing. https://search.proquest.com/openview/a9f97b38f980509daada53297ce261a1/1

Baumann, V. (n.d.). Rain-triggered lahar initiation in volcanic areas (Master's thesis). University of Geneva. https://archive-ouverte.unige.ch/download/8929e408-c9e6-4a82-b4f4-de554604b1f7

Janda, R. J., Daag, A. S., & Delos Reyes, P. J. (1996). *Assessment and response to lahar hazard around Mount Pinatubo, 1991 to 1993*. United States Geological Survey. https://pubs.usgs.gov/pinatubo/janda/

Pierson, T. C. (1992). *Immediate and long-term hazards from lahars and excess sedimentation in rivers draining Mt. Pinatubo, Philippines* (USGS Circular 1073). United States Geological Survey. https://books.google.com/books?id=9XDuAAAAMAAJ

Punongbayan, R. S., Rodolfo, K. S., Solidum, R. U., & Umbal, J. V. (n.d.). Assessment and response to lahar hazard. Retrieved from Academia.edu. https://www.academia.edu/download/53600980/Assessment_and_response_to_lahar_hazard_20170620-2065-13nofq8.pdf

Sambajon, S. D., Kobayashi, K., & Almorfe, S. T. (2024). Variability of soil characteristics around an active volcano, Mt. Mayon in the Philippines with special reference to the distance and direction from the crater. *Soil Science and Plant Nutrition.* https://doi.org/10.1080/00380768.2024.2317243

Tabios, G. Q. III (2020). *Water Resources Systems of the Philippines: Modeling Studies*. Springer. https://books.google.com/books?id=49fIDwAAQBAJ